Available online at www.sciencedirect.com
SCIENCE DIRECT
Journal of the European Ceramic Society 26 (2006) 187–192
www.elsevier.com/locate/jeurceramsoc

Oxidation of monolithic TiB_2 and TiB_2–20 wt.% $MoSi_2$ composite at 850 °C

T.S.R.Ch. Murthy[a], R. Balasubramaniam[a], B. Basu[a,*], A.K. Suri[b], M.N. Mungole[a]

[a] *Department of Materials and Metallurgical Engineering, Indian Institute of Technology (IIT), Kanpur 208016, India*
[b] *Material Processing Division, BARC, Mumbai, India*

Received 30 July 2004; received in revised form 14 October 2004; accepted 25 October 2004
Available online 19 January 2005

Abstract

The isothermal oxidation behavior of monolithic TiB_2 and TiB_2–20 wt.% $MoSi_2$ composite was evaluated at 850 °C in air. The monolithic TiB_2 exhibited continuous weight gain with increasing time. The TiB_2–$MoSi_2$ composite showed continuous weight gain till 16 h and afterwards the weight gain decreased markedly. The weight loss observed in composite after 16 h has been related to the formation and subsequent vaporization of MoO_3. The surfaces of the oxidized samples have been characterized by XRD and SEM. The XRD analysis indicated that the predominant phase present in the oxide was TiO_2 (rutile). Cracking of the surface scales was observed for the composite and monolithic TiB_2. Detailed SEM–EDS compositional analysis across oxide cross-section of the 64 h oxidized samples indicated enrichment of B_2O_3 on the surface of TiB_2 and SiO_2 in the case of the composite.

Keywords: Oxidation; TiB_2; TiB_2–$MoSi_2$; Scale characterization; Rutile

1. Introduction

Titanium diboride (TiB_2) is one of the important refractory borides.[1] A major limitation in widespread use of dense TiB_2 is its poor sinterability and its sensitivity to oxidation. Surface oxides like TiO_2, $TiBO_3$ and B_2O_3 are detrimental to densification of TiB_2 powders.[2,3] However, the densification is enhanced when non-metallic additives like SiC,[4,5] Si_3N_4,[6] AlN[7], and $MoSi_2$[8] are used.

In high temperature applications, oxidation resistance is an important property that needs to be critically considered. The oxidation mechanism of TiB_2 depends on the temperature, partial pressure of oxygen, time of exposure, porosity and the nature of sintering additives. In oxidation of TiB_2 powders, Kulpa and Troczynski[9] reported $TiBO_3$ and B_2O_3 formation at low temperatures (<400 °C), while TiO_2 and B_2O_3 formed at higher temperatures (600–900 °C). In case of oxidation of monolithic TiB_2, similar oxides form on the surface and the textured nature of TiO_2 has been reported.[10,11] The oxidation mechanism is governed by a diffusion mechanism up to 900 °C.[11] In case of TiB_2–2.5 wt.% Si_3N_4 composite,[12] the surface oxide consisted of an inner TiO_2 and outer B_2O_3 layer at lower temperature, while at higher temperature the surface was covered with only a thick crystalline TiO_2 layer. Parabolic kinetics was observed up to 900 °C during the oxidation of TiB_2–12.06 wt.% B_4C–2.1 wt.% Ni composite.[13] Highly textured TiO_2 (rutile) and crystalline B_2O_3 were observed in increasing amounts with increasing temperature.[13] The oxidation behavior of TiB_2-based cermets has also been investigated,[14–16] wherein the effect of the binder phase on oxidation nature has been clearly noted. When Si and Al based additives were added to TiB_2, oxidation resistance was enhanced due to formation of SiO_2 or Al_2O_3 on the surface.[4,7]

In a recent work, $MoSi_2$ was used as a sinter-additive to densify TiB_2 at a lower hot pressing temperature of 1700 °C.[8] The details of the processing and properties of the TiB_2–$MoSi_2$ composites can be found elsewhere.[8] The

* Corresponding author. Tel.: +91 512 2597771; fax: +91 512 2597505.
E-mail address: bikram@iitk.ac.in (B. Basu).

0955-2219/$ – see front matter © 2004 Elsevier Ltd. All rights reserved.
doi:10.1016/j.jeurceramsoc.2004.10.025

objective of present study was to evaluate the isothermal oxidation behavior of monolithic TiB_2 and TiB_2–$MoSi_2$ (20 wt.%) composite in air at 850 °C because this is the maximum service temperature for the application envisaged for these materials.[8] Several earlier oxidation studies on monolithic $MoSi_2$ have addressed the oxidation behavior at lower temperatures.[17–19]

2. Experimental procedure

The monolithic TiB_2 and TiB_2–$MoSi_2$ (20 wt.%) composites used in present study were fabricated by hot pressing at 1700 °C for 1 h and at 32 MPa in vacuum. The monolithic TiB_2 and TiB_2–$MoSi_2$ composite possessed densities of 88 and 95% ρth (theoretical density), respectively. The addition of $MoSi_2$ was beneficial in improving the sintered density of TiB_2. The relatively lower sintered density of the monolithic TiB_2 could be due to the lower hot pressing temperature. SEM images of the fracture surfaces of monolithic TiB_2 and TiB_2–$MoSi_2$ composite, hot pressed at 1700 °C, are shown in Fig. 1. The presence of pores can be easily distinguished in the structure. In the monolithic sample, only TiB_2 peaks were detected by X-ray diffraction (XRD) analysis. In the composite, in addition to TiB_2 and $MoSi_2$, the presence of titanium disilicide ($TiSi_2$) was identified in an electron probe micro analyzer and X-ray diffraction. This was further confirmed by transmission electron microscopy.[8] The formation of $TiSi_2$ can be attributed to limited reaction between matrix and dispersoids during hot pressing.

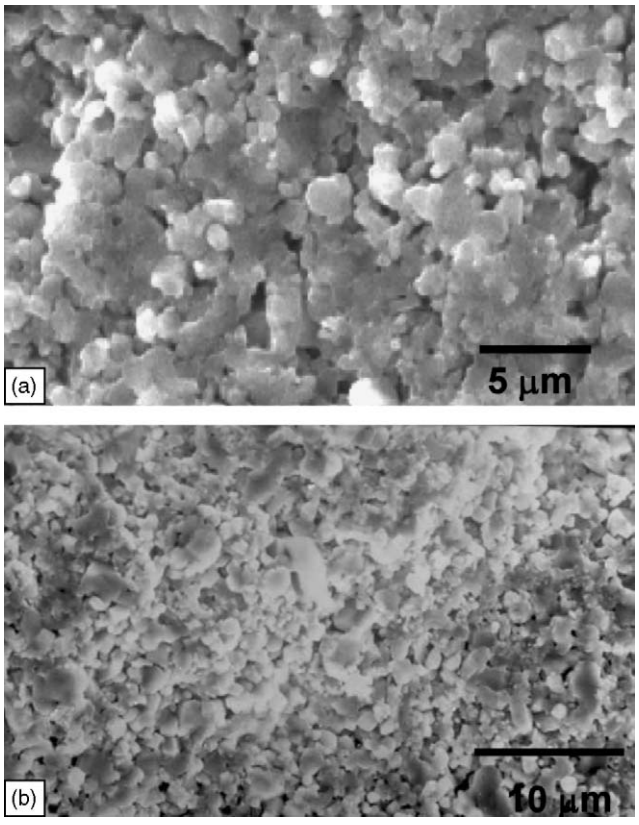

Fig. 1. SEM images of the fracture surfaces of the newly developed ceramics, hot pressed at 1700 °C for 1 h: (a) monolithic TiB_2 and (b) TiB_2–$MoSi_2$ composite.

Hot pressed pellets of diameter 10 mm were sectioned into 2 mm thick discs using high-speed diamond cutter. These discs were polished with emery papers (1/0, 2/0, 3/0, 4/0) and finally with diamond paste up to 1 μm finish. The polished discs were ultrasonically cleaned in acetone for 10 min.

Oxidation tests were conducted in a vertical tube furnace. In order to avoid oxidation during heating, the samples were directly inserted into the furnace after the furnace temperature reached 850 °C. Temperature was measured using a chromel–alumel thermocouple with an accuracy of ±10 °C. Samples were placed in an alumina crucible and suspended into the furnace. A total of eight samples, for each material, were oxidized for different time intervals (0.5, 1, 2, 4, 8, 16, 32, and 64 h) at 850 °C. The dimensions of the samples were accurately noted. Each sample was carefully weighed before and after exposure, to determine the weight change during the oxidation process.

The surfaces of the oxidized samples were characterized using XRD and scanning electron microscopy (SEM). XRD patterns were obtained from the surface of the oxidized samples using Cu Kα (λ = 1.5405 Å) radiation in a Rich-Seifert, 2000D diffractometer. The patterns were later analyzed using Diffrac^{Plus} software (Bruker Advanced X-ray Solutions, Germany) and JCPDF database. The morphology and nature of oxide layer was understood by observing the surface in a JSM-840A JEOL scanning electron microscope (SEM). The oxide cross-sections of the monolithic and composite samples after 64 h of oxidation were also studied. Elemental X-ray maps were obtained on the cross-sections of 64 h oxidized monolithic and composite. A compositional line scan was performed across the cross-section of 64 h oxidized composite using a FEI QUANTA 2000 HV SEM. Prior to SEM observation, the oxidized samples were sputter coated with a thin Au–Pd coating in order to obtain sufficient conductivity on the surface and avoid charging of the surface in the SEM.

3. Results and discussion

The weight gain data obtained during oxidation at 850 °C as a function of time for both monolithic TiB_2 and TiB_2–20% $MoSi_2$ composites are presented in Fig. 2a. In the case of monolithic TiB_2, the weight gained continuously with time. However, the weight gain of the composite was dependent on the exposure time. TiB_2–$MoSi_2$ composite exhibited continuous weight gain till 16 h, after which a significant drop in the weight gain was observed. In order to understand the kinetics of oxidation, the data were analyzed using the parabolic law, i.e.

$$\left(\frac{\Delta w}{A}\right)^2 = K_p t \quad (1)$$

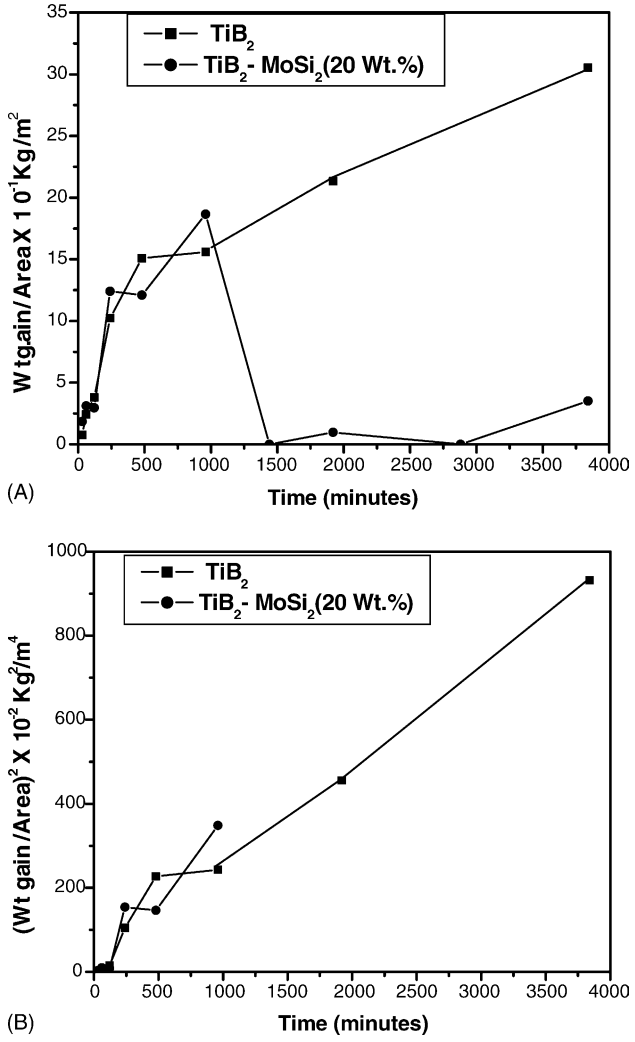

Fig. 2. (a) Weight gain curves for oxidation of monolithic TiB_2 and TiB_2–$MoSi_2$ (20 wt.%) composite in air at 850 °C. The lines joining the data points are for visual aid only. (b) Variation of $(\Delta w/A)^2$ as a function of time for the isothermal oxidation of monolithic TiB_2 and TiB_2–$MoSi_2$ (20 wt.%) composite in air at 850 °C. The lines joining the data points are for visual aid only.

where Δw is the change in weight; A, surface area of the sample; t, oxidation time and K_p, parabolic rate constant. For analysis, the data obtained only up to 16 h was utilized for the TiB_2–$MoSi_2$ composite. The weight gain curves as per the parabolic rate law are provided in Fig. 2b. The parabolic rate constants have been presented in Table 1 and they were similar for the oxidation of monolithic TiB_2 up to 64 h and of TiB_2–$MoSi_2$ composite up to 16 h. This indicates that the mechanism of oxidation in the case of composite was at least similar to that of monolithic TiB_2 up to 16 h of oxidation.

Table 1
Summary of rate constants processed from the data of the isothermal oxidation experiments (the data only up to 16 h was considered for composite material)

Material	$K_p \times 10^5$ (kg^2 m^{-4} s^{-1})	$K_m \times 10^4$	m
Monolithic TiB_2	4.087	2.246	1.414
(TiB_2–$MoSi_2$) composite	5.992	3.349	1.423

The parabolic rate constant determined in the present study for monolithic TiB_2 were about three orders of magnitude higher than that determined by Tampieri et al.[12] for oxidation of TiB_2 at 850 °C (6×10^{-8} kg^4 m^2 s^{-1}). The higher K_p obtained for the monolithic TiB_2 in the present study may be related to the higher amount of porosity. It can be noted here that the hot pressed condition used by Tampieri et al.[12] resulted in monolithic TiB_2 with a higher sintered density (98% ρth).

In order to understand the nature of oxidation, the data used in the parabolic law analysis above was also fit to the general rate equation

$$\left(\frac{\Delta w}{A}\right)^m = K_m t \quad (2)$$

where Δw is the change in weight; A, surface area of the sample; t, oxidation time and K_m, rate constant. These results are also tabulated in Table 1. The oxidation nature can be termed as paralinear, because the value of m was closer to 1.5 for both materials. Moreover, the nature of oxidation (up to 16 h) appears to be similar for both materials. The nature of oxidation changed after 16 h in the case of the composite (Fig. 2a) and this needed to be understood.

X-ray diffraction analysis (not shown) revealed that after oxidation, only crystalline rutile (TiO_2) (JCPDF 21-1276) could be unambiguously identified in both samples. The presence of B_2O_3 could be clearly confirmed in samples oxidized up to 4 h. Minor phases like $TiBO_3$, MoO_3, and SiO_2 could not be identified, although they have been reported to form in other studies.[4,9,12] This could be due to their low volume fraction in the surface oxide volume from where the XRD information was obtained or due to their possible presence as non-crystalline phases.

Scanning electron micrographs of the surface oxide scales of monolithic TiB_2 after oxidation at 850 °C for different times are presented in Fig. 3. The oxide surfaces were found to be severely cracked. The surface of the 64 h-oxidized sample appeared as if a liquid film was present on the surface. It may be due to the formation of liquid B_2O_3 during oxidation. The fusion point of B_2O_3 is ~500 °C and its boiling point is ~1100 °C.[14] It has also been reported that due to the small radius of the boron atom, it can diffuse easily to the surface during oxidation of TiB_2.[15,16]

The presence of glassy B_2O_3 could not have been determined by XRD studies possibly because of its non-crystallinity. In order to understand the possible formation of B_2O_3 on the surface of the oxide, the cross-section of the monolithic TiB_2 sample oxidized for 64 h was compositionally mapped for the elements Ti, B, and O in the SEM. Oxygen and titanium were found throughout the oxide scale, confirming that the oxide was indeed primarily composed of rutile (TiO_2). The boron map revealed that it was also distributed fairly uniformly throughout the oxide scale, although in much

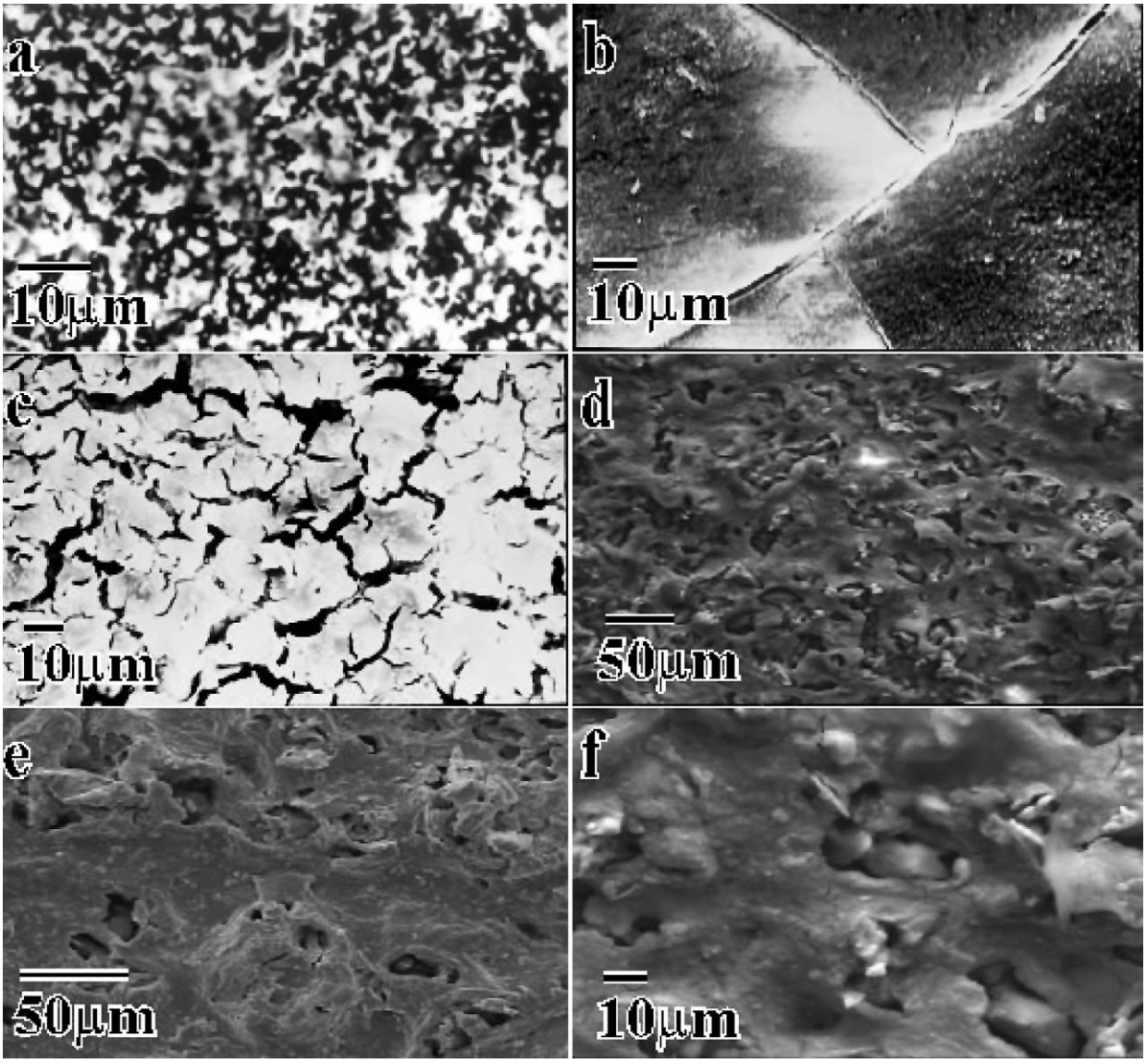

Fig. 3. SEM micrographs of surface of oxide scales of monolithic TiB_2 after oxidation at 850 °C for: (a) 0.5 h, (b) 1 h, (c) 4 h, and (d–f) 64 h.

lower concentration compared to TiO_2. However, there was a slight enhancement in its concentration towards the metal oxide–environment interface. Compositional analysis determined directly on the surface of the 64 h-oxidized sample provided strong signals for the presence of B. Therefore, it was concluded that the relative amount of B_2O_3 was higher on the surface of the oxide. In the case of monolithic TiB_2, the oxide was primarily composed of TiO_2 and possibly enriched with B_2O_3 on the surface.

The surface morphology of oxide scales on the composite has been presented in Fig. 4. Cracks were observed on the surface, which was relatively severe even for the sample oxidized for 1 h (Fig. 4a). The surface of the sample after oxidation for 16 h and 24 h indicated evidence for pesting (Fig. 4c–f). Pest behavior can be defined as disintegration of structure. $MoSi_2$ exhibits pest behavior at lower temperatures (400–600 °C), wherein $MoSi_2$ decomposes into MoO_3 and SiO_2.[17,18] The oxidation of $MoSi_2$ under these conditions can be described by the following reaction.

$$2MoSi_2 + 7O_2 \rightarrow 4SiO_2 + 2MoO_3 \uparrow \quad (3)$$

Pesting behavior in $MoSi_2$ has typically been associated with the formation of MoO_3 whiskers and SiO_2 clusters.[17–19]

In the present study, the presence of fine whiskers was clearly indicated at several locations on surface of the composite sample oxidized for 24 h (Fig. 4c–e). In fact, the microstructure presented in Fig. 4e indicates a structure similar to that reported by Chou and Nieh[17] and Hansson et al.[19] for the surface of oxidized $MoSi_2$, showing MoO_3 whiskers on top of discontinuous SiO_2 cluster. The protruding nature of MoO_3 whiskers has been proposed to open the structures and

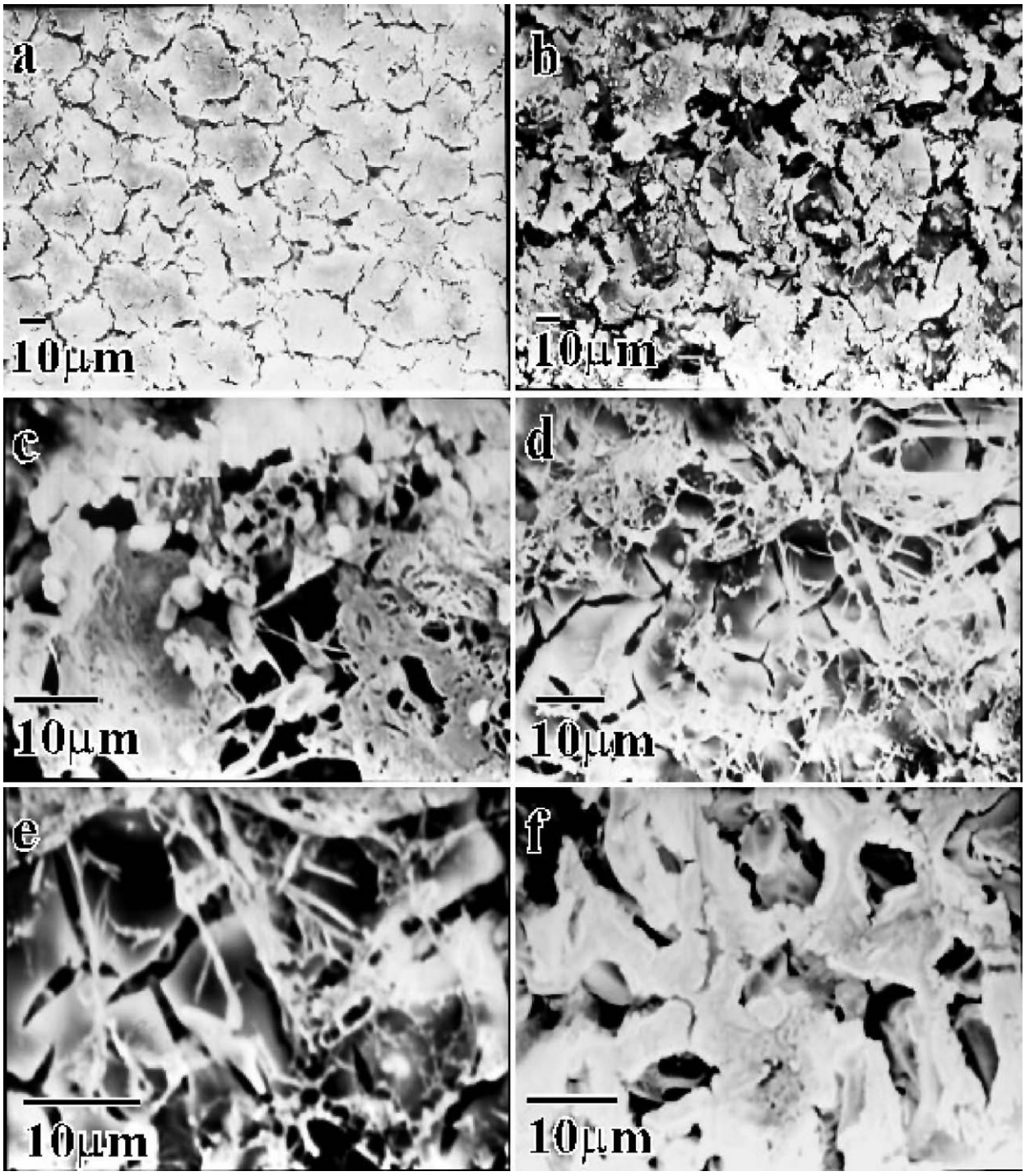

Fig. 4. SEM micrographs of surface of oxide scales of composite (TiB_2–$MoSi_2$) after oxidation at 850 °C for: (a) 1 h, (b) 16 h, (c–e) 24 h, and (f) 64 h.

accelerate the disintegration of $MoSi_2$.[17,18] The vapor pressure of MoO_3 is quite high at high temperature (9×10^{-3} Pa at 500 °C).[17] Therefore, the formation of volatile MoO_3 assists disintegration. The morphology of the whiskers observed on the composite surface in the present study indicated that the thickness of whiskers was less than 1 μm and the length varied from 5 to 20 μm.

Compositional analysis of the oxidized composite after 64 h oxidation at 850 °C indicated the presence of boron, titanium, silicon, and oxygen throughout the cross-section, while Mo was present only in traces. The outer surface layer of oxidized sample was enriched with SiO_2 at several locations. Tampieri et al.[11] have observed the formation of SiO_2 layer on the surface during the oxidation of Si_3N_4–TiB_2 (20 vol.%)

composite. The identification of SiO_2 and the almost near absence of Mo in the scale suggest that the non-protective nature of $MoSi_2$ oxidation may have resulted in the observed weight loss for the composite sample. Moreover, it has been reported that the formation of whisker MoO_3 and cluster SiO_2 on $MoSi_2$ occurs by nucleation and growth mechanism.[17] The rate-limiting step has been shown to be MoO_3 whisker formation. Therefore, the delayed weight loss behavior in case of composite sample can be related to the delay in formation of MoO_3 whiskers. Interestingly, MoO_3 formation is accelerated when oxygen exposure is limited and this condition would occur beneath the TiO_2 and B_2O_3 initially formed. With subsequent growth of MoO_3 and formation of SiO_2, the nature of oxidation for the composite changed from that observed with the monolithic TiB_2 (Fig. 2a).

Koh et al.[12] observed parabolic weight gain for TiB_2–2.5 wt.% Si_3N_4 composite exposed in air at 800 °C, while Graziani et al.[13] reported parabolic kinetics for TiB_2–20 vol.% B_4C composite up to 900 °C. In present study, paralinear kinetics were observed for monolithic and composite when exposed in air at 850 °C. Surface cracks were observed on the oxide in the present study. The thickness of the oxides on the surface of the monolithic and composite samples after 64 h oxidation at 850 °C was 150 and 25 μm. The presence of cracks in the oxide can result in control of the oxidation process by a diffusion controlled as well as phase boundary controlled reaction, thereby resulting in paralinear behavior.

4. Conclusions

The oxidation behavior of TiB_2 and TiB_2–20% $MoSi_2$ composite were investigated in air at 850 °C and the following conclusions can be drawn:

a) In case of monolithic TiB_2, the weight gain increased continuously with time. TiB_2–$MoSi_2$ composite exhibited continuous weight gain only up to 16 h, after which there was a considerable drop in the weight gain. Analysis of oxidation data using parabolic rate constant indicated slightly improved oxidation resistance for TiB_2 compared to the composite. Crystalline rutile (TiO_2) could be identified unambiguously on the oxidized surfaces of both TiB_2 and composite by XRD analysis. The surface scales on oxidized TiB_2 were severely cracked. The formation of B_2O_3 during oxidation of TiB_2 and its enrichment on the surface was indicated by SEM analysis.
b) In the case of TiB_2–$MoSi_2$ composite, whisker type MoO_3 oxide formation on the surface was noted after 24 and 64 h of oxidation. Enrichment of Si was also noted on the surface of the composite sample after 64 h of oxidation. The oxidation behavior in the case of the composite has been related to the nucleation and growth of MoO_3 and SiO_2 in the oxide.

Acknowledgment

The financial support by the Board of Research in Nuclear Science (BRNS) of Department of Atomic Energy (DAE), Government of India is gratefully acknowledged.

References

1. Telle, R. and Petzow, G., Strengthening and toughening of boride and carbide hard material composites. *Mater. Sci. Eng. A*, 1988, **105/106**, 97–104.
2. Baik, S. and Becher, P. F., Effect of oxygen contamination on densification of TiB_2. *J. Am. Ceram. Soc.*, 1987, **70**(8), 527–530.
3. Einarsrud, M., Hagen, E., Pettersen, G. and Grande, T., Pressureless sintering of titanium diboride with nickel, nickel boride, and iron additives. *J. Am. Ceram. Soc.*, 1997, **80**(12), 3013–3020.
4. Torizuka, S., Sato, K., Nishio, H. and Kishi, T., Effect of SiC on interfacial reaction and sintering mechanism of TiB_2. *J. Am. Ceram. Soc.*, 1995, **78**(6), 1606–1610.
5. Torizuka, S. and Kishi, T., Effect of SiC and ZrO_2 on sinterability and mechanical properties of titanium nitride, titanium carbonitride and titanium diboride. *Mater. Trans. JIM*, 1996, **37**(4), 782–787.
6. Ho Park, J., Koh, Y., Kim, H., Hwang, C. and Kong, E., Densification and mechanical properties of titanium diboride with silicon nitride as sintering aid. *J. Am. Ceram. Soc.*, 1999, **82**(11), 3037–3042.
7. Li, L. H., Kim, H. E. and Kang, E. S., Sintering and mechanical properties of titanium diboride with aluminum nitride as a sintering aid. *J. Eur. Ceram. Soc.*, 2002, **22**, 973–977.
8. Murthy, T. S. R. Ch., Shrivastava, A., Basu, B., Balasubramaniam, R., Suri, A. K., Subramanian, C. *et al.*, Processing and properties of novel TiB_2-based composites, *J. Am. Ceram. Soc.*, submitted for publication.
9. Kulpa, A. and Troczynski, T., Oxidation of TiB_2 powders below 900 °C. *J. Am. Ceram. Soc.*, 1996, **79**(2), 518–520.
10. Tampieri, A. and Bellosi, A., Oxidation of monolithic TiB_2 and of Al_2O_3–TiB_2 composite. *J. Mater. Sci.*, 1993, **28**, 649–653.
11. Tampieri, A., Landi, E. and Bellosi, A., On the oxidation behavior of monolithic TiB_2 and Al_2O_3 and Si_3N_4–TiB_2 composites. *J. Thermal Anal.*, 1992, **38**, 2657–2668.
12. Koh, Y. H., Lee, S. Y. and Kim, H. E., Oxidation behavior of titanium boride at elevated temperatures. *J. Am. Ceram. Soc.*, 2001, **84**(1), 139–141.
13. Graziani, T., Landi, E. and Bellosi, A., Oxidation of TiB_2–20 vol.%B_4C composite. *J. Mater. Sci. Lett.*, 1993, **12**, 691–694.
14. Barandika, M. G., Echeberria, J. J. and Castro, F., Oxidation resistance of two TiB_2-based cermets. *Mater. Res. Bull.*, 1999, **34**(7), 1001–1011.
15. Lavrenko, V. A., Chuprov, S. S., Umanskii, A. P., Protsenko, T. G. and Lugovskaya, E. S., High-temperature oxidation of composite materials based on titanium diboride. *Soviet Powder Met. Metal. Ceram.*, 1987, 761–762.
16. Singh, M. and Wiedemeier, H., Chemical interactions in diboride-reinforced oxide-matrix composites. *J. Am. Ceram. Soc.*, 1991, **74**(4), 724–727.
17. Chou, T. C. and Nieh, T. G., New observations of $MoSi_2$ pest at 500 °C. *Scripta Metall. Mater.*, 1992, **26**, 1637–1642.
18. Wirksus, C. D. and Wilder, D. R., High-temperature oxidation of molybdenum disilicide. *J. Am. Ceram. Soc.*, 1966, **49**(4), 173–177.
19. Hansson, K., Halvarsson, M., Tangb, J. E., Pompec, R., Sundberg, M. and Svensson, J. E., Oxidation behaviour of a $MoSi_2$-based composite in different atmospheres in the low temperature range (400–550 °C). *J. Eur. Ceram. Soc.*, 2004, **24**, 3559–3573.